

Single-Particle Density of the Renormalized Fermi-Gas Model

Sudip Kumar Ghosh

Saha Institute of Nuclear Physics, Calcutta 9, India

and

Aparesh Chatterjee

Calcutta University and Saha Institute of Nuclear Physics, Calcutta 9, India

(Received 2 May 1972)

It is well known that the nuclear single-particle level density g_{obs} , obtained from statistical nuclear reactions, does not follow the behavior of a free Fermi gas; previous attempts to reproduce g_{obs} have largely been empirical. We have used the properties of our renormalized gas model (RGM) to deduce an approximate analytic expression for our model density g_{RGM} . We study the consequence of the concept of momentum anisotropy in the phase space of the RGM system relative to the isotropic distribution of the free Fermi gas. We find that our model is a very suitable one to fit in with this concept. With fair accuracy, we find that $g_{\text{RGM}} = g_{\text{obs}}$ throughout the range of stable nuclei, $50 \leq A \leq 250$. The effects of specific model interaction energies (the single-particle combinatorial effects, the pairing, deformation, and Coulomb effects) are all observed in appropriate regions in desired strengths. All these effects are strongly dominated by the prescribed shell structure and its state-mixing and occupation dependence.

1. INTRODUCTION

The single-particle level density g at the Fermi surface ϵ of a nucleus, or its associated level-density parameter $a = \pi^2 g / 6$, is a basic parameter in the nuclear statistical-type model. A proper definition of g or a is necessary for evaluating the nuclear level densities. The most common form of nuclear model in use in this context is the simple free Fermi-gas model¹ – a system of A noninteracting particles confined to move in a spherical volume $V_0 = 4\pi r_0^3 A / 3$ with an isotropic momentum distribution in a rectangular well of arbitrary depth. Assuming that a continuous density-of-state function $g_0(\epsilon)$ exists, the total phase space occupied by the system in its ground state is the volume-momentum product,

$$A = \int_0^{\epsilon_0} g_0(\epsilon) d\epsilon = \int_0^{\epsilon_0} 4V_0(2\pi\hbar)^{-3} 4\pi p^2 \frac{dp}{d\epsilon} d\epsilon = 4V_0\Omega_0(2\pi\hbar)^{-3}, \quad (1)$$

where ϵ_0 is the Fermi energy, Ω_0 is the momentum volume, and \hbar is the action constant; the factor 4 with V_0 appears on account of the spin and isospin of the nucleons. The Fermi energy ϵ_0 and the single-particle level density g_0 at ϵ_0 for such a system are¹

$$\epsilon_0 = (9\pi/8)^{2/3} \hbar^2 / 2m r_0^2, \quad (2)$$

and

$$g_0 \equiv g_0(\epsilon_0) = 3A/2\epsilon_0 = 6a_0/\pi^2, \quad (3)$$

where m and r_0 are the nucleon mass and radius, respectively. We note that ϵ_0 is a universal constant (independent of the number of particles A of the system) and that g_0 is a simple linear function of A . We take this as our reference system and use the subscript naught for quantities (e.g., V_0 , Ω_0 , ϵ_0 , g_0 , a_0 , etc.) of this system.

A real nuclear system, however, is not a system of free fermions. There are often discernible shell, deformation, pairing, isospin, and Coulomb effects in the ground state of a nucleus. Experimentally derived values of the level-density parameter $a_{\text{exp}} = \pi^2 g_{\text{exp}} / 6$ often reveal^{2,3} most of these effects. By its very nature, the free Fermi-gas model can in no way reproduce these features. One attempts to include these effects in several possible ways.⁴⁻⁷ The early approaches^{4,5} are semiempirical exercises of statistical level counting. Attempts have been made^{6,7} to estimate the “shell corrections” in the mass formula (average liquid-drop energy surface) from an ansatz of the free-gas model. These attempts⁴⁻⁷ are briefly discussed in Sec. 2.

A recent self-consistent approach includes the short- and long-range parts of the nuclear interactions on the free Fermi-gas model. It describes the statistical properties of a model system from the nuclear interaction energies in a realistic manner. The model has been named the renormalized gas model (RGM). In this work, we shall concern ourselves mainly with various aspects of the single-particle level density of the RGM system, and shall compare them with experiments.

2. PAST STUDIES ON THE NUCLEAR SINGLE-PARTICLE DENSITY

The earliest attempts to understand the observed features^{2,3} of the nuclear single-particle level density are those of Newton⁴ and Cameron.⁵ They both realized that the region of interest of $g(\epsilon)$ is near the free Fermi-gas surface ϵ_0 .

Newton defined⁴ an average density \bar{g}_0 near ϵ_0 as

$$\bar{g}_0 = \frac{\int_{-\infty}^{+\infty} g(\epsilon) \ln[1 + \exp - (\epsilon - \epsilon_0)/t] d\epsilon}{\int_{-\infty}^{+\infty} \ln[1 + \exp - (\epsilon - \epsilon_0)/t] d\epsilon}, \quad (4)$$

where t is the thermodynamic temperature of the free-gas system at an excitation energy U obeying the relations

$$t = (6U/\pi^2 g_0)^{1/2} = (U/a)^{1/2}. \quad (5)$$

Newton's shell effects are contained in $g(\epsilon)$, since his average spacing d in a given shell degeneracy ($2j_v + 1$) is greater than the splitting between the j_v substates. He took

$$g(\epsilon) = g_n + g_p = 2(j_n + j_p + 1)/d, \quad (6)$$

where n and p refer to neutron and proton configurations, respectively. For a spherical nucleus of radius $R = r_0 A^{1/3}$, $d \propto R^{-2} \propto A^{-2/3}$, and (6) may be written as

$$g(\epsilon) = 2\alpha(j_n + j_p + 1)A^{2/3}, \quad (7)$$

where α is a constant. The choice of j_n and j_p was made⁴ from an early form of shell model. An iterative procedure was used to average $g(\epsilon)$ to obtain \bar{g}_0 in (4). In effect, j_n and j_p were replaced by their averages \bar{j}_n and \bar{j}_p , respectively, to define \bar{g}_0 as

$$\bar{g}_0 = 2\alpha(\bar{j}_n + \bar{j}_p + 1)A^{2/3}. \quad (8)$$

The adjustable constant α was determined from the nature of variation of $gA^{2/3}$ with the mass number A . Since j_n and j_p are small near the closed shells, Newton predicts the magic shell effect (drop in the magnitude of g) prior to the positions of actual magic particle configurations.

Cameron⁵ averaged the single-particle spacings instead of the densities. He used his semiempirical mass formula together with empirically introduced shell and pairing corrections $S(Z, N)$ and $P(Z, N)$, additive for Z protons and N neutrons:

$$S(Z, N) = S(Z) + S(N), \quad (9)$$

$$P(Z, N) = P(Z) + P(N).$$

$P(Z)$ or $P(N)$ were set as zero for odd values of Z or N . Treating the problem of exciting the nu-

cleons from the Fermi surface as one of adding particles (rather than lifting a nucleon to an excited state), Cameron wrote the proton and neutron spacings as

$$d(Z) = M(Z, A) - 2M(Z - 1, A - 1) + M(Z - 2, A - 2), \quad (10a)$$

$$d(N) = M(Z, A) - 2M(Z, A - 1) + M(Z, A - 2), \quad (10b)$$

to be evaluated near the valley of β stability. These orbit spacings were then averaged similarly to Newton's density-averaging procedure; the reciprocal of these spacings defined his single-particle level density.

Myers and Swiatecki⁶ deduced a four-parameter liquid-drop-model (LDM) semiempirical mass equation containing exponential shape and range dependences of nuclear masses with the deformation parameter α :

$$M(Z, N, \alpha) = M_{\text{LDM}}(Z, N, \alpha) + Cs(Z, N) \exp[-\langle(\delta R)^2\rangle_{\text{av}}/\alpha^2]. \quad (10c)$$

A staircase "shell" function $s(Z, N)$ along the line of β stability was defined. The free Fermi-gas model was invoked to determine the shell corrections with three parameters. Their mass formula was fitted to about 1200 masses and 240 quadrupole moments. Although the single-particle level density was not explicitly deduced, the change in the Fermi energy due to shell bunching of states was used as the shell correction $s(Z, N)$.

Strutinsky⁷ pointed out that the distribution of the single-particle states as a function of the ground-state deformation in the Nilsson diagram⁸ clearly shows an inhomogeneity in energy space. In most phenomenological models (e.g., the LDM), this distribution is assumed to be uniform. Strutinsky argued that the predicted inhomogeneous distribution of states of soluble models seems to define regions of stable deformation and regions of closed shell-like configurations at certain deformations. One may treat this inhomogeneity as an average "shell" correction on the homogeneous liquid-drop energy surface. The single-particle state density was taken as

$$g_v(E) = (\pi\gamma)^{-1/2} \sum_v \exp\{[E - E_v(\eta)]^2/\gamma^2\}, \quad (11)$$

where γ is the energy region (shell interval) over which the averaging is performed, and $E_v(\eta)$ represents the nucleon levels at a given Nilsson deformation parameter⁸ η . An oversimplified Gaussian distribution of levels (with $\gamma \approx 0.15\hbar\omega$, where $\hbar\omega$ is the Nilsson oscillator energy) was used to calculate $g_v(E)$.

3. RGM PHASE SPACE FOR SPHERICAL SYSTEMS

The RGM⁹ treats a nuclear system as an ensemble of interacting fermions. It measures all nuclear interaction energies from the particle-invariant free-gas reference Fermi surface ϵ_0 . The Fermi energy of a given nucleus ϵ_F is considered to be a shift of ϵ_0 . The magnitude of the shift $\delta\epsilon = \epsilon_F - \epsilon_0$ is computed as an adiabatic sum of the long- and short-range nuclear interaction energies.

The RGM appears to give a fair account of fission energy partitions,¹⁰ fast-neutron ($n, 2n$) reaction cross sections,¹¹ prompt fission fragment γ decay,¹² and independent mass yield in fission.¹³ The computational details of $\delta\epsilon$ are briefly reviewed in Sec. 4.

An inhomogeneous distribution of single-particle level density requires a complete reformulation of the phase-space analysis. We note from (1) that the free-gas system has an isotropic momentum distribution $\Omega_0 = \int 4\pi p^2 dp$. Nuclear interactions will distort this to an anisotropic one. Introduction of an anisotropy in momentum space is thus equivalent to the introduction of suitable interactions on our reference free-gas system.¹ Assuming that the continuous density-of-states functions $g_0(\epsilon)$ and $g(\epsilon)$ may be defined as functions of nucleon kinetic energy ϵ in both cases, one may compare the densities for the two systems at their respective Fermi surfaces with the same number of particles A . This last constraint (viz., the total number of particles is the same in both cases) is simply a restatement of the RGM condition that ϵ_0 is the hypothetical reference energy of the nucleus. Since we have already elaborated the concept of momentum anisotropy in a separate note,¹⁴ we stress here the parallel between the RGM approach and the phase-space analysis, while touching upon the salient points of the latter. The total phase space of a spherical system of A interacting particles now reads

$$A = \int_0^{\epsilon_F} g(\epsilon) d\epsilon = 4V\Omega(2\pi\hbar)^{-3}, \quad (12)$$

where V and Ω are the space and momentum volumes of the interacting system. The factor 4 has the same origin as in Sec. 1. On switching off the nuclear interactions, (12) reduces to (1) and ϵ_F goes to ϵ_0 in accordance with the RGM hypothesis.

In case of spherical nuclei, $V = V_0 = 4\pi r_0^3 A/3$; setting Ω to be numerically equal to Ω_0 , we get

$$\int_0^{\epsilon_F} 4\pi p^2 (dp/d\epsilon) d\epsilon = \int_0^{\epsilon_F} f(p) (dp/d\epsilon) d\epsilon, \quad (13)$$

where $f(p)$ is an elementary momentum surface of the interacting system; $f(p)$ represents a non-

spherical surface under the constraint $\epsilon_F \neq \epsilon_0$. A deformed surface $f(p)$ is a direct consequence of the nuclear interactions being introduced in our reference free-gas system.

The expansion used¹⁵ to treat the nuclear shape deformations (restricting to small, axially symmetric, volume-conserving deformations) is written in terms of a radius vector R of the deformed object expanded¹¹ around the spherical radius R_0 as

$$R = R_0 \left[1 + \sum_{n=1}^{\infty} \beta_n P_n(\cos\theta) \right] \lambda_B^{-1}, \quad (14)$$

where λ_B is a volume-conserving constant, and other symbols have their usual meanings. Our RGM satisfies all conditions for making a similar expansion of the momentum volume Ω . We had found⁹⁻¹⁴ that (i) the RGM correction $\delta\epsilon$ is small ($\delta\epsilon < \epsilon_0$) and hence the momentum anisotropy will be small, (ii) the RGM momentum volume is conserved and hence a deformation expansion is possible, and (iii) an expansion around the RGM reference momentum $p_0 = (2m\epsilon_0)^{1/2}$ seems to be an ideal choice. We try an expansion

$$P = p_0 \left[1 + \sum_{n=1}^{\infty} \alpha_n P_n(\cos\theta) \right] \lambda^{-1}. \quad (15)$$

The maximum momentum radius should correspond to the Fermi momentum $p_F = (2m\epsilon_F)^{1/2}$. Since P varies with the polar angle θ , we have to determine for what value of θ the observable Fermi momentum p_F of the RGM system exists. Introducing a variable y as a function of the local momentum P , we have

$$Y = p_0 \left[1 + \sum_{n=1}^{\infty} \alpha_n P_n(\cos\theta) \right] \lambda^{-1}, \quad (16)$$

where the volume-conserving constant λ has the form¹⁵

$$\lambda^3 = \frac{1}{2} \int_{\cos\theta=-1}^1 \left[1 + \sum_{n=1}^{\infty} \alpha_n P_n(\cos\theta) \right]^3 d(\cos\theta). \quad (17)$$

We are to show the exact functional dependence of y on p and the connection between Y and p_F .

Retaining only the lowest symmetric term α_2 , we write (15) approximately as

$$Y \approx p_0 [1 + \alpha_2 P_2(\cos\theta)] \lambda^{-1} = a + bx^2, \quad (18)$$

where

$$\begin{aligned} a &= p_0(1 - \alpha_2/2)/\lambda, \\ b &= 3p_0\alpha_2/2\lambda, \\ x &= \cos\theta, \end{aligned} \quad (18')$$

and λ is obtained from (17) as

$$\lambda^3 = 1 + 3\alpha_2^2/5 + 2\alpha_2^3/35. \quad (18'')$$

Since we have introduced both α_2 and $\delta\epsilon$ as our measures of deformation, we relate them as

$$\alpha_2 = \delta\epsilon/\epsilon_0 = (\epsilon_F/\epsilon_0) - 1. \quad (19)$$

The total momentum volume Ω in (13) may be written as

$$\Omega = \int_0^{\epsilon_F} F(y) \frac{dy}{d\epsilon} d\epsilon = \int_{\theta=0}^{\pi} \int_{y=0}^Y \int_{\phi=0}^{2\pi} y^2 \sin\theta d\theta dy d\phi. \quad (20)$$

The total phase space, from (12) and (20), is

$$A = \int_0^{\epsilon_F} \frac{4VF(y)}{(2\pi\hbar)^3} \frac{dy}{d\epsilon} d\epsilon = \int_{x=0}^1 \int_{y=0}^{a+bx^2} \frac{16\pi V}{(2\pi\hbar)^3} y^2 dx dy \quad (21)$$

from which we obtain

$$g(\epsilon) = \frac{dA}{d\epsilon} = 4V(2\pi\hbar)^{-3} F(y) \frac{dy}{d\epsilon}. \quad (22)$$

In (21), we make a necessary change in the order of integration since the upper limit of y integration is itself a function of x . The integration, using (18), gives

$$A = \frac{16\pi V}{(2\pi\hbar)^3} \left[\int_{y=0}^{a+b} y^2 dy - \int_{y=a}^{a+b} y^2 \left(\frac{y-a}{b} \right)^{1/2} dy \right]. \quad (23)$$

The two integrands may be combined into a common integral within common limits of the first integral ($y=0$ to $y=a+b$) by making the required change in the second integrand.¹⁸ The form of (23) is then

$$A = \frac{16\pi V}{(2\pi\hbar)^3} \int_0^{a+b} \left[y^2 - \frac{b}{a+b} \left(\frac{by}{a+b} + a \right)^2 \left(\frac{y}{a+b} \right)^{1/2} \right] dy, \quad (24)$$

whence the function $F(y)$ in (22) is solved as

$$F(y) = 4\pi \left[y^2 - \frac{b}{a+b} \left(\frac{by}{a+b} + a \right)^2 \left(\frac{y}{a+b} \right)^{1/2} \right]. \quad (25)$$

We ascertain the relationship between y and p (or ϵ) at this stage with the help of boundary conditions (21) and (24). Noting that

$$\epsilon = 0 \quad \text{when } y = 0,$$

and

$$\epsilon = \epsilon_F \quad \text{when } y = a + b, \quad (26)$$

we get, from (19),

$$\begin{aligned} \epsilon_F &= \epsilon_0(1 + \alpha_2), \\ a + b &= p_0(1 + \alpha_2)/\lambda = p_0\epsilon_F/\lambda\epsilon_0 \end{aligned} \quad (27)$$

at the maximum limits of y and ϵ . Replacing the limits by the actual variables, we have

$$\begin{aligned} y &= p_0\epsilon/\lambda\epsilon_0, \\ \frac{dy}{d\epsilon} &= p_0/\lambda\epsilon_0, \end{aligned} \quad (28)$$

which automatically satisfy the conditions (26).

The single-particle density may now be written

from (22), (25), and (28) as

$$\begin{aligned} g(\epsilon) &= \frac{16\pi V}{(2\pi\hbar)^3} \frac{p_0}{\lambda\epsilon_0} \\ &\times \left[y^2 - \frac{b}{a+b} \left(\frac{by}{a+b} + a \right)^2 \left(\frac{y}{a+b} \right)^{1/2} \right], \end{aligned} \quad (29)$$

whence the single-particle level density $g(\epsilon_F)$ at the RGM Fermi surface ϵ_F may be simplified to

$$g = g(\epsilon_F) = \frac{2g_0(\epsilon_F/\epsilon_0)(1 - \frac{1}{2}\alpha_2)}{\lambda^3}. \quad (30)$$

The observed Fermi momentum p_F corresponds to the maximum of Y ($Y_{\max} = a + b$) at $\theta = 0$.

4. PHASE SPACE OF DEFORMED NUCLEI

No special properties of the RGM system need be invoked to treat the problem of permanently deformed nuclei. The RGM energy correction $\delta\epsilon$ now includes the energy of deformation $-E_\beta$ at the ground-state deformation β , and a change in momentum distribution is indicated. The space volume of a deformed nucleus is obtained from

$$V = \int_{\theta'=0}^{\pi} \int_{r=0}^{R(\theta')} \int_{\phi'=0}^{2\pi} r^2 \sin\theta' d\theta' dr d\phi' = V_0. \quad (31)$$

A change in the order of integration as before (Sec. 3) gives $V = \int_0^R f(r, \beta_2) dr$ with the upper limit R now independent of θ' . The total phase space may be written as

$$A = \frac{1}{(2\pi\hbar)^3} \int_{r=0}^R \int_{\epsilon=0}^{\epsilon_F} f(r, \beta_2) \mathfrak{F}(\epsilon, \alpha_2) dr d\epsilon, \quad (32)$$

retaining only the lowest-order symmetric-deformation terms in both cases, and defining a new function $\mathfrak{F}(\epsilon, \alpha_2)$ instead of $F(y)$ in (25). The assumption of Sec. 3, viz., that the nuclear shape and the momentum distributions are separately conserved, leads to a physically untenable situation according to the formalism developed. We note that since the limits of the double integral are constants, each integral is to be treated separately, but the radial integral again yields just V_0 . If we conserve the total phase space as a single entity, we expect that one kind of deformation will reflect on the other. This in essence requires defining a new set of dynamical coordinates to describe the problem [in the notation of (32), the limits R and ϵ_F , and the parameters α_2 and β_2 , will be interrelated.] In lieu of this complicated procedure, we introduce an alternative simple approach, which involves small adjustments of our

mathematical procedure (with perhaps less rigor), but none of principles.

A shape-deformed nucleus with a symmetric ground-state deformation β_2 is more stable than a spherical one; as Mosel and Greiner¹⁷ have phrased it, the "binding energy of deformation," E_β , will reduce the kinetic energy of the system by the amount E_β . Since our α_2 is directly proportional to the RGM correction $\delta\epsilon$, we define a new deformation α_2 in case of permanently deformed nuclei as

$$\alpha_2 = (\delta\epsilon - E_\beta)/\epsilon_0 = [(\epsilon_F - E_\beta)/\epsilon_0] - 1, \quad (33)$$

instead of (19). Our limits in (27) are now redefined as

$$a + b = (p_0/\lambda\epsilon_0)(\epsilon_F - E_\beta), \quad (34)$$

from which the variable y in (28) may be written

$$y = (p_0/\lambda\epsilon_0)(\epsilon - E_\beta), \quad (35)$$

with the same value of $dy/d\epsilon$ in (28). The boundary conditions in (26) are now slightly changed; although at $y = a + b$, the upper limit of ϵ remains ϵ_F as before, at $y = 0$, we have the new lower limit

$\epsilon = E_\beta$. (24) now reads

$$A = \int_{E_\beta}^{\epsilon_F} \frac{4V}{(2\pi\hbar)^3} F(y) \frac{dy}{d\epsilon} d\epsilon = \int_{E_\beta}^{\epsilon_F} g'(\epsilon) d\epsilon, \quad (36)$$

where $g'(\epsilon)$ has the explicit form

$$g'(\epsilon) = \frac{16\pi V}{(2\pi\hbar)^3} \frac{p_0}{\lambda\epsilon_0} \left\{ \frac{p_0^2(\epsilon - E_\beta)^2}{\lambda^2\epsilon_0^2} - \frac{b}{a+b} \left[\frac{bp_0(\epsilon - E_\beta)}{(a+b)\lambda\epsilon_0} + a \right]^2 \left[\frac{p_0(\epsilon - E_\beta)}{(a+b)\lambda\epsilon_0} \right]^{1/2} \right\}. \quad (37)$$

Using Landau's translation theorem,¹⁶ (36) may be written as an integral within limits of zero and $\epsilon_F - E_\beta$, instead of that of E_β and ϵ_F ; necessary changes are then required in (37). The final density $g(\epsilon)$ is obtained, again changing the limits of integration from zero to ϵ_F , along with the concurrent changes in the integrand, as discussed in deducing (24). The final result, after these manipulations, is

$$g(\epsilon) = \frac{dA}{d\epsilon} = \frac{16\pi V}{(2\pi\hbar)^2} \frac{p_0(\epsilon_F - E_\beta)}{\lambda\epsilon_0\epsilon_F} \left[\frac{p_0^2\epsilon^2(\epsilon_F - E_\beta)^2}{\lambda^2\epsilon_0\epsilon_F^2} - \frac{b}{a+b} \left(\frac{bp_0\epsilon(\epsilon_F - E_\beta)}{(a+b)\lambda\epsilon_0\epsilon_F} + a \right)^2 \left(\frac{p_0\epsilon(\epsilon_F - E_\beta)}{(a+b)\lambda\epsilon_0\epsilon_F} \right)^{1/2} \right]. \quad (38)$$

The single-particle level density $g(\epsilon_F)$ at ϵ_F of a deformed nuclear system is obtained by putting proper limits in (38):

$$g_{\text{RGM}} = g(\epsilon_F) = \frac{2g_0(\epsilon_F - E_\beta)^2(1 - \frac{1}{2}\alpha_2)}{\epsilon_0\epsilon_F\lambda^3} \approx 2g_0 \left(1 - \frac{2E_\beta}{\epsilon_F} \right) \left(\frac{1 - \frac{1}{2}\alpha_2}{\lambda^3} \right), \quad (39)$$

which is approximately

$$g_{\text{RGM}} \approx 2g_0 \left(1 - \frac{2E_\beta}{\epsilon_0 + \delta\epsilon} \right) \left(1 + \frac{\delta\epsilon}{\epsilon_0} \right) \left(1 - \frac{(\delta\epsilon - E_\beta)^2}{2\epsilon_0^2} \right) \left(1 + 0.6 \frac{(\delta\epsilon - E_\beta)^2}{\epsilon_0^2} \right)^{-1}, \quad (39')$$

neglecting the term cubic in α_2 in λ .

Switching off the nuclear shape deformation interaction ($E_\beta = 0$), the momentum deformation α_2 and the constant λ in (33) to (38) will fall back to the corresponding quantities α_2 and λ of (18) to (29); the density (39) goes back to (30). Comparison of these two equations shows the important result¹⁸ that the deformation energy E_β reduces the effect of momentum anisotropy in $g(\epsilon_F)$. A test of this prediction is made later in Secs. 6 and 9 in regions of permanently deformed nuclei.

5. OUTLINE OF THE RGM AND ITS COMPUTATIONAL PROCEDURE

Use of (39) to compute the single-particle level density $g(\epsilon_F)$ requires knowledge of $\delta\epsilon$ and ϵ_F . Assuming sufficient adiabaticity between different nuclear interactions, the main RGM interactions amongst ν interacting particles are the single-particle energy corrections and those due to pairing and deformation. The Rosenzweig type of single-particle shell correction¹⁹ f tends to unbind the midshell nuclei, while the Belyaev-type quasiparticle interactions²⁰ tend to bind them:

$$\epsilon_F = \epsilon_0 + \delta\epsilon = \epsilon_0 + f - \Delta^2/G - E_\beta. \quad (40)$$

The pairing interaction correction $E_p = \Delta^2/G$, the gap correction Δ , and the deformation energy E_β , may be estimated from the Belyaev model²⁰ if the input parameters of the model are uniquely defined. We assume that corrections due to extra-core neutrons and protons are additive:

$$\delta\epsilon = \sum_\nu \delta\epsilon_\nu = \delta\epsilon_n + \delta\epsilon_p.$$

The Rosenzweig combinatorial correction¹⁹ is of the form

$$f \approx \frac{1}{g_0} \frac{\mathfrak{n}_b^2}{12} - \frac{1}{2}(\nu - \frac{1}{2}\mathfrak{n}_b)^2, \quad (41)$$

where $\mathfrak{n}_b = 2j_\nu + 1$ is the shell degeneracy and ν is the number of particles in the shell \mathfrak{n}_b . Near closed shells, f changes sign and goes negative, and the Belyaev interactions tend to go to zero; one may interpret the closed-shell RGM system to have a binding energy $f_s = -\mathfrak{n}_b^2/24g_0$ relative to the free Fermi gas. In regions of pure shell-model states, the combinatorial correction (41) predicts a parabolic dependence with the number of particles ν .

In regions of strong state mixing, one may define effective Rosenzweig functions¹⁰⁻¹⁴ f_m and f_i for the major shell m and the i th subshell, respectively, in terms of the corresponding degen-

eracies N_m and N_i :

$$f_m = g_0^{-1} \left[\frac{N_m^2}{12} - \frac{1}{2} (n_m - \frac{1}{2} N_m)^2 \right], \quad (42)$$

$$f_i = g_0^{-1} \left[\frac{N_i^2}{12} - \frac{1}{2} (n_i - \frac{1}{2} N_i)^2 \right],$$

where $N_m = \sum_{i=1}^k N_i$, k being the total number of subshells contained in m . The main problem is to sum up the two interactions in (42) suitably in the form $f = \lambda f_m + \mu f_k$. A particularly suitable simple choice is¹⁰⁻¹⁴

$$f = (\frac{1}{2}) [(f_m/k) + f_i], \quad (43)$$

which has the special advantage of using all quantities from the shell model; a further desirable feature is that at the start (or end) of a major shell m , the effects of the following (or preceding) $k-1$ subshells are suppressed, so that the effect of the k th subshell ($k=i=1$) alone is felt; the choice (43) then reduces to $f = \frac{1}{2}(f_m + f_k)$.

An energy normalization at this stage is necessary to introduce the quasiparticle interactions. We assume that the transition $\epsilon_0 \rightarrow \epsilon'$ due to the Rosenzweig f interactions alone brings the system back to a system having a level spectrum of equidistant spacings.

The pairing correction E_p and the gap correction Δ are given by¹⁹

$$E_p = \Delta^2/G, \quad G_z = 52/Z, \quad G_N = 46/N, \quad (44)$$

and

$$\Delta = [(\epsilon_b - \epsilon_a)/2 \sinh \eta] (1 - \chi^2)^{1/2}, \quad (45)$$

where ϵ_b and ϵ_a are the energies at the shell boundaries, b and a , respectively, and

$$\eta = 1/\bar{g}G, \quad \bar{g} = \frac{1}{2}(g_b + g_a), \quad \chi = 1 - 2\nu/\mathfrak{n}_b, \quad (46)$$

\bar{g} being the mean density, g_b and g_a the level densities at b and a , and $(1 - \chi^2)$ is the occupation factor (χ is the occupation amplitude).

The equilibrium deformation energy E_β at the ground-state deformation β has been calculated¹¹ following Bès²¹ based on the Nilsson⁸ level scheme

$$E_\beta \approx \frac{1}{2}(\epsilon_b - \epsilon_a) \Lambda(\eta), \quad (47)$$

where the Belyaev occupation parameter $\Lambda(\eta)$ is

$$\Lambda(\eta) = \frac{1}{8}\mathfrak{n}_b(1 - \chi^2) \left\{ (1 - \frac{1}{3}\xi^2)\gamma(\eta) - 2\epsilon\chi[\gamma(\eta) \coth \eta - \frac{2}{3}] \right\}, \quad (48)$$

$$\xi = (g_b - g_a)/(g_b + g_a),$$

$$\gamma(\eta) = \coth \eta (1 - 2\eta/\sinh 2\eta). \quad (49)$$

The Coulomb contribution to the nuclear deforma-

tion energy E_B is in the form of an expansion

$$E_C(\beta) = \frac{5}{4\pi} E_{C_0} \sum_n \frac{n-1}{2n+1} \beta_n^2 \approx E_{C_0} (1 - \beta^2/4\pi - \dots), \quad (50)$$

where E_{C_0} is the Coulomb energy of a spherical nucleus. The deformation parameter β may be calculated using the relationship of Mosel and Greiner^{12,17}

$$E_B \approx \frac{1}{2} C \beta^2, \quad C \approx C_0 (1 - \delta\epsilon'/\epsilon_0), \quad (51)$$

where $\delta\epsilon'$ is the RGM correction due to Rosenzweig and pairing interactions alone, and C_0 is the stiffness coefficient of the nuclear system.

In our computations, the input parameters of the Belyaev interaction energies (44), (45), and (47), were fixed from (41)–(43), and no further adjustments were made. They are thus free from arbitrary parameters and themselves form a self-consistent set of parameters. The constant C_0 in (51) was taken as¹² ~ 320 MeV.

Our computed a parameters have been plotted in Figs. 1 and 2 in the stable nuclear mass range 50

$\leq A \leq 250$. We expect different features of our RGM (viz., magic shell and subshell effects, mid-shell effects, odd-even effects, and deformation effects) to show up in these predictions.

6. COMPARISON WITH EXPERIMENTS

The experimental a parameters are mostly derived from the analysis of slow-neutron resonance data or from nuclear-reaction cross sections using the equidistant-spacing-model level-density formula. Neutron resonance data have been used by Newton⁴ in 52 nuclei, by Ross²² in 50 nuclei, by Erba, Facchini, and Saetta-Menichella² in 100 nuclei, by Lang²³ in 83 nuclei, and by Facchini and Saetta-Menichella³ in 189 nuclei. In addition, Ref. 2 analyzed 31 nuclei from fast-neutron (n, n') and (n, p) cross sections and 5 nuclei from (p, n) reactions; these usually show wider fluctuations of a values compared to the slow-neutron (n, γ) resonances.

In these analyses, the level-density function $\rho(U, J)$ of a nucleus at an excitation U is used in

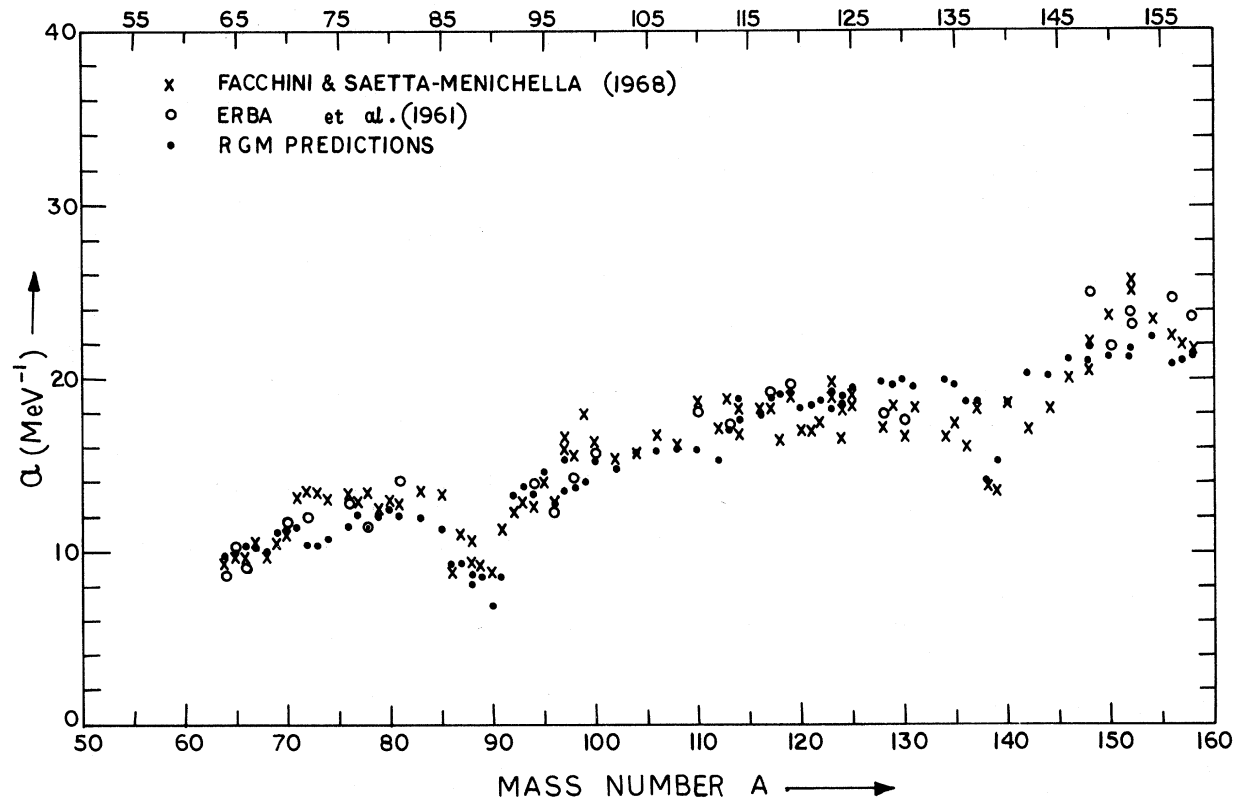


FIG. 1. A comparison of experimental a parameters (Refs. 2, 3) with our predicted values in the medium-mass region, $50 \leq A \leq 160$. Note that the general trend, and the magnitudes, agree reasonably satisfactorily throughout this mass region from our model formulation using the single-particle schemes of Ref. 8.

the usual exponential form¹

$$\rho(U, J) = \frac{6^{1/4} \exp 2(aU)^{1/2} (2J+1)}{12g^{1/4} U^{5/4} 2(2\pi)^{1/2} \sigma^3} \exp[-J(J+1)/2\sigma^2], \quad (52)$$

where σ is the spin cutoff parameter. It is customary⁴ to introduce an odd-even correction Δ in U :

$$U = E_n + Q - \Delta, \quad (53)$$

where E_n is the incident neutron energy and Q is the reaction energy (Q value).

In the analysis of the slow-neutron resonance data, the observed level spacing D_{obs} is usually taken to be

$$D_{\text{obs}}^{-1} = \frac{1}{2} [\rho(U, J = I + \frac{1}{2}) + \rho(U, J = I - \frac{1}{2})] \quad \text{for } l = 0, \quad (54)$$

$$= P_J \sum_J \rho(U, J) \quad \text{for } l > 0, \quad (54')$$

where l is the orbital angular momentum of the neutron, I is the ground-state spin of the target nucleus, and the parity weight factor $P_J = 1$ or 2 ,

depending on one or both kinds of parities being observed. Fluctuations of D_{obs} should be weakly reflected in the a parameter, since D_{obs}^{-1} is an exponential function of a in (52) and (54). However, there is considerable discrepancy in the deduced a parameters from different sources. The two sets of analysis of the Milan group^{2,3} agree well and usually predict slightly higher a values than the rest. We have included both these sets for comparison purposes in Figs. 1 and 2.

In Fig. 1, the region of medium-weight nuclei $50 \leq A \leq 160$ has been covered. Our comparison starts beyond the $1f_{7/2}$ shell for neutrons and protons ($A > 63$), where $N/Z \geq 1$, and the neutron and proton systems just start to behave differently. Calculations have been made for all nuclei tabulated in Refs. 2 and 3, to allow a point-by-point comparison. The over-all fit in general trend and magnitudes is reasonably satisfactory (<25%) throughout and <10% in 53 cases out of 81 nuclei, i.e., in about 65% cases). In the region $73 < A < 76$, our computed values show a trend opposite to the experimental values. There is considerable uncertainty of the neutron subshell filling order in the Ga-Ge-As region (see Sec. 7). One finds a good

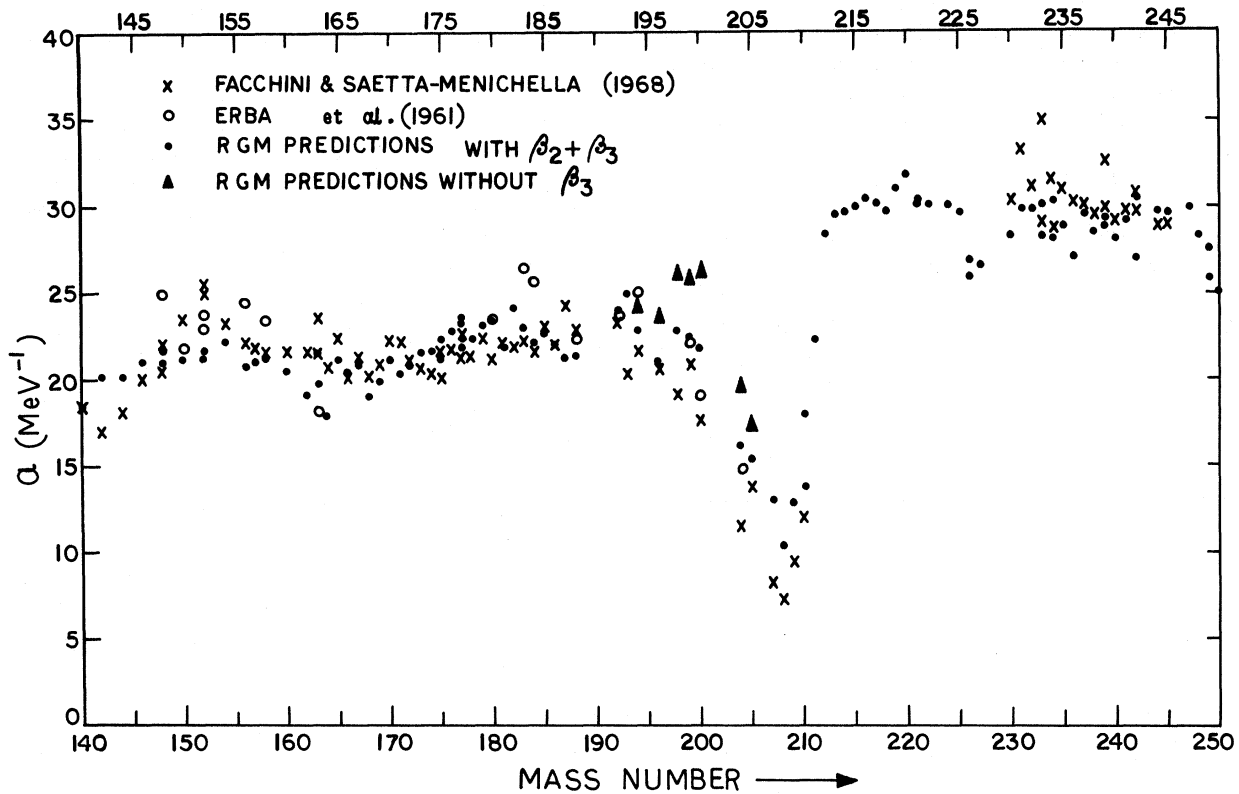


FIG. 2. A comparison of the experimental a values (Refs. 2, 3) with our predictions in the heavy-mass region, $140 \leq A \leq 250$. We have used the more appropriate single-particle scheme of Ref. 36 in this region; the fit throughout is again reasonably satisfactory.

agreement in the observed and calculated dips in the mass-90 region (Rb, Sr, Y, and Zr isotopes). Slight discrepancies exist around $A \sim 98$ and $A \sim 110$ (Mo isotopes), mainly due to the assumed contributions of $l=0$ and $l=1$ neutrons only in the experimental analysis; since the local neutron states are $2d_{5/2}$ and $1g_{7/2}$, inclusion of the effect of neutrons of higher angular momenta is expected to bring down the values nearer to our predictions. Similar argument also applies in the $A \sim 75$ region. A good fit with this predicted decrease is observed also in the $A \sim 138$ region (followed by a rise up to $A = 150$).

Figure 2, the region of heavy nuclei, $140 \leq A \leq 250$, compares the experimental analysis^{2,3} of 108 nuclei with our predictions. We note that a misfit occurs for ^{150}Sm , ^{152}Sm , ^{152}Eu , and ^{163}Dy . The experimental values themselves differ considerably in this region, as shown in Table I. In the permanently deformed region (rare earths), our model deformation energy E_β in (47) plays a vital role in reducing the magnitude of the a parameter, as is experimentally found. The Coulomb contribution ΔE_C in E_β has to be included to obtain realistic results.

Another interesting region in Fig. 2 is that of transitional nuclei (Pt, Au, and Hg isotopes). These nuclei are known to have considerable amounts of asymmetric deformation β_3 at or near the ground state in addition to the symmetric deformation $\beta(\equiv\beta_2)$. This matter is further discussed in Sec. 9.

A large local drop in the a parameter is observed in the ^{207}Pb , ^{208}Pb , and ^{209}Pb isotopes, near the $Z = 82$, $N = 126$ configuration. Our theory and experiments agree within 30% here.

After a sharp rise up to $A = 212$, our calculations predict a plateau in the $212 \leq A \leq 225$ region and a $\sim 20\%$ drop in the Ra-Ac region (mass ~ 226). Un-

fortunately, there are no experimental data to compare with in this region. Comparison is again possible at $230 \leq A \leq 245$, where the three sets of numbers^{2,3,14} agree within $\sim 15\%$. A drop is predicted beyond $A \approx 246$, but no comparison with experiments is possible.

7. SHELL AND SUBSHELL EFFECTS

Our predicted and the experimental trends both show magic shell effects at $N = 28, 50, 82$, and 126 and at $Z = 28, 50$, and 82 .

From Figs. 1 and 2, one may argue that there are no prominent proton and neutron subshell effects in the a parameters. The experimental information has traditionally been interpreted in this way. Our calculations show that although the subshell effects seem to be unimportant in magnitude, their real absence would imply a much higher predicted a value in several regions (particularly in the midshell regions of a major shell) with much different slopes in the general trends. This is specially true for the neutron subshells in ^{88}Zn ($1f_{5/2}$), ^{98}Mo ($2d_{5/2}$), ^{112}Cd ($1g_{7/2}$), ^{152}Sm ($2f_{7/2}$), and ^{168}Er ($1h_{9/2}$) nuclei, and for protons in the Ge, Sr, Ba, and Gd isotopes. In these cases, the subshell effects of the other kind of nucleons interfere to keep the local a parameter to a lower observed value.

In our calculations, we had assumed a proton shell closure at $Z = 40$, and have obtained the fit shown in Fig. 1. In the Nilsson scheme,⁸ the subshell gap in the mass-90 region amounts almost to a major shell gap. The effect in $Z = 50$ near the mass-130 region is thereby relatively weakened; in this region of the $1h_{11/2}$ neutron midshell, only weak neutron subshell effects are observed. In our notation (43), $k = 1$ in the $1g_{9/2}$ proton shell, $40 \leq Z \leq 50$.

TABLE I. Comparison of the experimental and predicted a parameters near the mass ~ 155 region (rare earths). Note discrepancies (10–15%) in the two analyses (Refs. 2 and 3). The role of the model deformation energy E_β in our calculated values is shown in the last two columns.

Nucleus	Ref. 2		Ref. 3		$a_{\text{RGM}}(\text{MeV}^{-1})$	
	D_{obs} (MeV)	a_{expt} (MeV^{-1})	D_{obs} (MeV)	a_{expt} (MeV^{-1})	Without E_β	With E_β
$^{150}_{82}\text{Sm}_{68}$	3.3×10^{-6}	21.77	2.4×10^{-6}	23.61	25.10	21.10
$^{152}_{82}\text{Sm}_{70}$	1.3×10^{-6}	23.05	1.0×10^{-6}	25.56	25.50	21.10
$^{152}_{83}\text{Eu}_{69}$	7.3×10^{-7}	23.88	6.5×10^{-7}	25.05	25.70	21.60
$^{156}_{84}\text{Gd}_{72}$	2.1×10^{-6}	24.48	1.9×10^{-6}	22.45	26.00	20.65
$^{158}_{84}\text{Gd}_{74}$	2.0×10^{-6}	23.49	5.5×10^{-6}	21.60	26.40	21.20
$^{162}_{66}\text{Dy}_{96}$	1.2×10^{-6}	23.63	2.2×10^{-6}	21.69	26.60	18.90
$^{163}_{66}\text{Dy}_{97}$	2.0×10^{-4}	18.17	1.0×10^{-4}	21.39	26.60	18.70

The statistical model of nuclear reactions predicts from (52) a low reaction cross section for a nucleus with lower a value. In a systematic analysis²⁴ of the shell effects in the (n, α) reaction cross sections with 14-MeV neutrons, described in terms of the Rosenzweig shell interaction¹⁹ alone, a subshell effect in the Ga-Ge-As region was predicted²⁵; this was later experimentally confirmed by Rao and Fink.²⁶ Similar effects are expected in the mass-88, -125, and -190 regions, and are indeed observed,²⁷ for instance at $A \sim 125$ ($1h_{11/2}$ neutron subshell).

8. ODD-EVEN EFFECTS

Neither the experimental data nor our predictions reveal any strong odd-even mass effects in Figs. 1 and 2. Our predicted values include both the interaction $P = \Delta^2/G$ and the pairing-gap correction Δ . These corrections attain their maximum values in the midshells. The magnitudes of these two together are $\sim 20\%$ of the total correction $\delta\epsilon$ in (40), and hence are numerically unimportant beyond the region of light nuclei ($A > 60$).

From the experimental data analysis, Newton⁴ pointed out that the observed level spacings D_{obs} in slow-neutron resonances do not exhibit any marked odd-even effect. One expects, however, that for thermal and slow neutrons, where the excitation energy U of the system is put equal to the neutron binding energy B_n , the residual nucleus should show rather strong odd-even effects. This point has been illustrated by Malishev,²⁸ who argues that the odd-even effects present in B_n should be strongly reflected in the level-density parameter. Newton⁴ suggested that the odd-even effect should be removed by measuring the excitation energy from a fictitious ground state such that

$$U = B_n - \Delta. \quad (55)$$

Neutron energies $50 < E_n < 100$ keV introduce a further small correction in B_n so that

$$U_{\text{eff}} = B_{\text{eff}} - \Delta = B_n + \frac{1}{2} E_n - \Delta, \quad (56)$$

which takes the place of (53) in the use of the level-density formula (52). The Δ values in (55) and (56) are usually taken from various mass formulas. Erba, Facchini, and Saetta-Menichella,² Gilbert and Cameron,²⁹ and Facchini and Saetta-Menichella³ used Δ values from the mass formula of Cameron and Elkin.³⁰ Malishev²⁸ used the values of Nemirovskii and Adamchuk³¹ deduced from the odd-even mass difference including the Coulomb and surface-energy corrections.

Our RGM Δ values, obtained from the Belyaev formulation, behave differently from the Δ values of Refs. 5, 28, and 29. Our values go to zero at

shell closure points because of their dependence on the occupation factor $(1 - \chi^2)$ in (45). The Δ 's of Nemirovskii and Adamchuk³¹ and of Cameron and Elkin,³⁰ however, have finite values at shell closures. Table II compares some of these values. The main discrepancies occur at or near the shell-closure positions, as discussed above. If we use the RGM Δ values for computing the a parameters from D_{obs} , the changes in the a values are only a few percent ($< 10\%$); the nature of the general trend in Figs. 1 and 2 is hardly affected by this substitution.

9. DEFORMATION EFFECTS

We recall that the model deformation energy E_β in (47) contains the Coulomb contribution $E_C(\beta)$, given by (50). They both go to zero for closed-shell nuclei which are stable in their spherical shapes. In the midshell nuclei, both model energies contribute, due to the symmetric deformation parameter $\beta (= \beta_2)$. This is indeed reflected in our theoretical estimates of the a parameters. Neglect of E_β will considerably enhance the magnitudes of the local a values (by $\sim 30\%$), as shown in a few sample comparisons in Table I. The Coulomb contribution $E_C(\beta)$ accounts for $\sim 15\%$ of this effect.

TABLE II. A partial comparison of RGM pairing-gap corrections Δ with those of Nemirovskii and Adamchuk (Ref. 31) and Cameron and Elkin (Ref. 30).

Nucleus	Ref. 31			Ref. 30 Δ	RGM		
	Δ_p	Δ_n	Δ		Δ_p	Δ_n	Δ
⁶⁴ ₃₀ Zn ₃₄	1.34	1.67	3.01	2.47	0.91	1.23	2.14
⁷² ₃₂ Ge ₄₀	1.72	2.15	3.87	2.79	1.09	0.76	1.85
⁸⁰ ₃₄ Se ₄₆	1.76	1.70	3.46	3.00	1.42	1.06	2.48
⁸⁸ ₃₈ Sr ₅₀	1.43	1.55	2.98	2.17	0.87	0	0.87
⁹² ₄₀ Zr ₅₂	1.31	0.92	2.23	1.92	0	0.41	0.41
⁹⁶ ₄₂ Mo ₅₄	1.68	1.18	2.86	2.40	1.83	0.58	2.41
¹⁰⁶ ₄₆ Pd ₆₀	1.18	1.32	2.50	2.59	1.86	0.93	2.79
¹¹⁸ ₅₀ Sn ₆₈	1.51	1.17	2.68	2.34	0	0.63	0.63
¹²⁶ ₅₂ Te ₇₄	1.27	1.46	2.73	2.23	0.59	0.89	1.48
¹³⁸ ₅₆ Ba ₈₂	0.98	0.96	1.94	2.43	0.92	0	0.92
¹⁴⁴ ₆₀ Nd ₈₄	1.38	0.99	2.37	1.94	0.97	0.61	1.58
¹⁵² ₆₂ Sm ₉₀	1.80	1.52	3.32	2.32	0.97	0.30	1.27
¹⁶² ₆₆ Dy ₉₆	0.86	0.98	1.84	1.62	1.23	0.43	1.66
¹⁷² ₇₀ Yb ₁₀₂	0.76	0.78	1.54	1.37	1.18	0.57	1.75
¹⁸² ₇₄ W ₁₀₈	0.54	0.71	1.25	1.45	0.93	0.58	1.51
¹⁹⁴ ₇₈ Pt ₁₁₆	1.47	1.14	2.61	1.55	0.40	0.45	0.85

The transitional nuclei are separately considered in Table III. Here, the asymmetric octupole deformation β_3 (in our approximate RGM treatment) goes to increase the "Coulomb deformation energy of binding,"

$$E_C(\beta + \beta_3) \approx (E_{C_0}/4\pi)[\beta^2 + 10\beta_3^2/7], \quad (57)$$

and this will increase the total deformation energy ($E_\beta + E_{\beta_3}$); the net result is an increased binding in these nuclei due to the combined deformations with a concurrent reduced magnitude of the a parameter, as shown in Fig. 2 and Table III, in the mass-195 region. Cohen³² has argued that for these nuclei, β_3 is almost as large as the symmetric deformation β ; our theoretical estimate, which gives the best fit with observations in this region, supports Cohen's conjecture. We may compare the two cases, $\beta_3 \approx \beta$ (black dots), and $\beta_3 \approx 0$ (triangles) in Fig. 2.

The model deformation energy enters twice in (39), once through the Fermi energy ϵ_F and once again through the momentum deformation parameter α_2 . The shape deformation of a nucleus thus plays a dual role in the momentum space. On the one hand, it redefines the upper limit of the momentum distribution by reducing the magnitude of ϵ_F and on the other, it readjusts the momentum shape by decreasing the magnitude of the anisotropy of such an interacting system. One which fits the experimental a values is the one in which this dual role is incorporated. This clearly illustrates the insufficiency of adjusting the "deformed" Fermi energy ϵ_F alone in these regions without a corresponding alteration in the momentum distribution.

Another interesting consequence of the deformation effects is found in the heaviest elements (Ra to Cf). A local subdip in the a parameters in the Ra-Ac region is not due to any shell or subshell closure effects, but is due to the presence of large

deformation energies (5 to 6 MeV). This corroborates the conjecture of Strutinsky⁷ that a stable (closed-shell-like) configuration exists in highly deformed nuclei; recast in our formulation (Sec. 4), large deformation energies reduce both the Fermi energy ϵ_F and the anisotropy of the momentum distribution α_2 to attain a stability.

10. DISCUSSIONS, SUMMARY, AND CONCLUSIONS

Several interesting consequences of the RGM show up clearly in the observed trends of the single-particle level densities. The specific RGM interaction effects have been discussed in Secs. 7 to 9. The main point we have learned is that the properties of the RGM system are governed primarily by the form of the shell model used. We have seen that the subshell mixing, occupation, pairing, and shape-deformation effects depend critically on this prescription. The pairing-interaction effects get considerably reduced in intensity in the heaviest stable nuclei. The nuclear shape-deformation effects gradually gain in intensity with increase in mass number, and show up characteristic effects in rare earths and light actinides; the Coulomb contribution to the deformation energy, and the presence of asymmetric deformations towards the end of a deformed major shell, are both strongly felt in these regions.

Two things happen when a subshell closure occurs in the midshell of highly deformed nuclei. The RGM correction $\delta\epsilon$ is reduced on account of the subshell closure itself, and the presence of large deformation energies further reduces the momentum anisotropy (and the Fermi energy ϵ_F). A valley in the rare-earth region, $A \sim 165$, is due to this combined effect. A similar thing happens in the actinide region, $A \sim 226$. These corroborate the Strutinsky hypothesis that regions of large deformations sometimes behave like closed-shell configurations.

The Rosenzweig shell correction f becomes double valued at magic configurations. A configuration of a closed shell \mathfrak{n} is also a point where the next available shell \mathfrak{n}' is completely open. We have, somewhat artificially, chosen the representation that the shell \mathfrak{n}' starts with the particle $\nu_{\mathfrak{n}'} = 1$, $\nu_{\mathfrak{n}'} = 0$ being equivalent to the closure of the previous shell \mathfrak{n} with $\nu_{\mathfrak{n}} = \mathfrak{n}$. The other possible representation does not agree with the experimental trends.

The odd-even mass effects are hardly observable in the single-particle level densities since such effects are usually small in magnitude.

We may raise a basic question: Is it possible to find a nuclear species which behaves like a free

TABLE III. Comparison of the experimental and predicted a parameters for nuclei near $A \sim 196$ (transitional nuclei).

Nucleus	a expt (MeV ⁻¹)	Reference No.	a_{RGM} with		
			$\beta_3 = 0$	$\beta_3 = 0.75\beta_2$	$\beta_3 = \beta_2$
¹⁹³ ₇₈ Pt ₁₁₅	20.19	3	24.90	22.90	20.75
¹⁹⁶ ₇₈ Pt ₁₁₈	20.62	3	23.60	22.60	20.40
¹⁹⁸ ₇₉ Au ₁₁₈	19.13	3	26.10	24.50	22.25
¹⁹⁹ ₈₀ Hg ₁₁₉	21.95	2	25.80	24.50	22.30
	20.68	3			
²⁰⁰ ₈₀ Hg ₁₂₀	19.01	2	26.20	25.10	23.00
	17.62	3			

gas? One may argue that when there is an accidental cancellation of RGM interaction energies, $\delta\epsilon \approx 0$, the system will behave as a free gas (cf. Sec. 1) in the sense that (a) its ground state will coincide with the free-gas Fermi energy ϵ_0 , and (b) its single-particle level density of equidistant spacings will be $g_0 = 3A/2\epsilon_0$. We note that it is possible to find nuclei in which $\delta\epsilon \sim 0$. Such nuclei occur near closed-shell configurations; near here, the model pairing and deformation interactions are small negative quantities, and the Rosenzweig interaction f changes sign (goes negative to positive, from the shell closure point towards midshell, cf. Sec. 5). The condition $\delta\epsilon \sim 0$ is then equivalent to $f \sim 0$, which gives $\nu_{gr} \sim \mathfrak{n}/12$; hence, for a just open large orbital angular momentum state with one or two particles, the system is expected to behave as a pseudofree gas. Such nuclei, however, will not have the approximate free-gas a parameter $a_0 = \pi^2 A/4\epsilon_0$, but will have $a \sim 2a_0$. The factor 2 in (30) and (39) arises mainly from our choice of the definition (19), where the momentum deformation α_2 is assumed to vary quadratically with the Fermi momentum p_F . An assumed linear variation does not reproduce the realistic behavior. Further, the gross average \bar{a}_{exp} (smoothing over all structure effects in Figs. 1 and 2) does not show a mean slope $\pi^2/4\epsilon_0$ with the mass number A , but appears to have a mean slope $\pi^2/2\epsilon_0 \lesssim \frac{1}{8}$. We also note that our RGM formulation in Sec. 6 predicts that the model a values reach the lowest limit $\sim a_0$ near the doubly magic Pb nucleus. Usually, the observed values lie close to, but smaller than, $2a_0$, due to the form of y in (28) and (35) or of a in (30) and (39).

The average, maximum, and minimum magnitudes of $\delta\epsilon$ in the region of stability are ~ 3 , ~ 7 , and ~ -2 MeV, if we take $\epsilon_0 \approx 31.0$ MeV following Cindro.³³ These numbers give binding energies ~ 7 , ~ 3 , and ~ 12 MeV, if we take the nuclear potential \mathcal{V} corresponding to $\hbar\omega = 41A^{-1/3}$ MeV following Nilsson.⁸ If the state-mixing or deformation effects were absent in heavy midshell nuclei, their binding energies would have gone to zero (or even positive).

An extrapolation of the formalism is possible to calculate the single-particle level densities of superheavy nuclei. This requires the knowledge of the shell structure of these nuclei. This information is now available in the form of several alternatives,³⁴⁻³⁶ and the most suitable form to choose is unknown. We have calculated the a values using all three schemes.

A detailed comparison with experiments appears in Fig. 3. The scheme of Rost³⁵ shows well-separated $1i_{13/2}$ and $2f_{7/2}$ proton subshells in contrast with the schemes of Seeger³⁴ and Nilsson *et al.*,³⁶

where these two states lie very close. A possibility of subshell mixing thus exists in the two latter schemes, which are essentially identical in general features in the mass region $210 \leq A \leq 260$. If we take the subshells to be unmixed, good fit with experimental data³ is obtained in this region using all the three schemes. Subshell mixing in the schemes of Refs. 34 and 36 will decrease a_{RGM} to about 60% of a_{obs} in the $^{238}_{93}\text{Np}$, $^{239}_{94}\text{Pu}$, $^{240}_{94}\text{Pu}$, $^{241}_{94}\text{Pu}$, $^{242}_{94}\text{Pu}$, $^{242}_{95}\text{Am}$, $^{244}_{95}\text{Am}$, and $^{245}_{96}\text{Cm}$ nuclei. We thus conclude from Fig. 3 that subshells in this region, while they may have small energy separations, re-

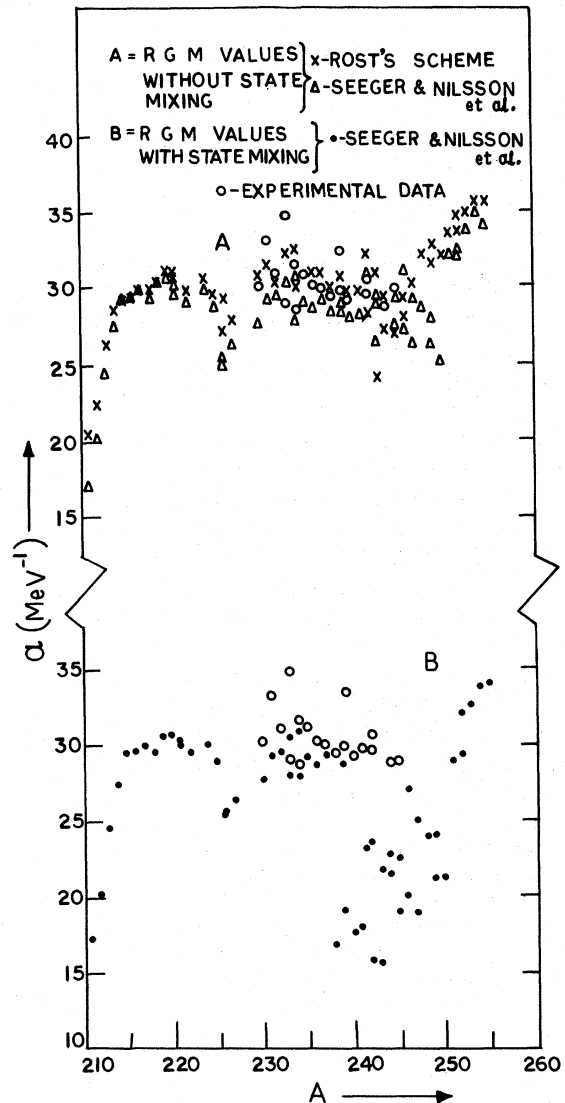


FIG. 3. A comparison of our predicted a parameters using different single-particle schemes (Refs. 34-36) with and without state-mixing effects. The few experimental data (Refs. 2, 3) shown as O in the mass range $230 \leq A \leq 245$ seem to favor all the three alternative schemes if the state-mixing effects in this mass region are ignored.

main unmixed. Using Rost's scheme, the fits beyond $A = 250$ (superheavy nuclei) worsen³⁷; further, the well-known neutron subshell closure effect,

found in the binding-energy systematics,³⁸ at $N = 152$, does not appear.

ACKNOWLEDGMENTS

It is a pleasure to thank Professor Nikola Cindro in Zagreb, and Professor Norbert Rosenzweig in Albany, for helpful discussions. Our sincere thanks are due Dr. Ratna Sarkar and Dr. Swapna Mukherjee of this institute for partial collaboration in this work. One of us (A.C.) wishes to thank Swapan Kumar Das of Surendranath College, Calcutta, for his help in computer programming.

¹H. A. Bethe, Phys. Rev. 47, 633, 747 (1935); 50, 332, 977 (1936); Rev. Mod. Phys. 9, 69 (1937); T. Ericson, Advan. Phys. 9, 425 (1960); A. Bohr and B. R. Mottelson, *Nuclear Structure* (Benjamin, New York, 1969), Vol. 1, Chap. 2, p. 281.

²E. Erba, U. Facchini, and E. Saetta-Menichella, Nuovo Cimento 22, 123 (1961).

³U. Facchini and E. Saetta-Menichella, Energia Nucl. 15, 24 (1968); U. Facchini, private communication.

⁴T. D. Newton, Can. J. Phys. 34, 804 (1956); 35, 1400 (1957).

⁵A. G. W. Cameron, Can. J. Phys. 36, 1040 (1958).

⁶W. D. Myers and W. J. Swiatecki, Nucl. Phys. 81, 1 (1966).

⁷V. M. Strutinsky, Nucl. Phys. A95, 120 (1957); V. M. Strutinsky and H. C. Pauli, in *Proceedings of the Second International Atomic Energy Symposium on Physics and Chemistry of Fission, Vienna, Austria, 1969* (International Atomic Energy Agency, Vienna, Austria, 1969), p. 155.

⁸S. G. Nilsson, Kgl. Danske Videnskab. Selskab, Mat.-Fys. Medd. 29, No. 1 (1955).

⁹A. Chatterjee, unpublished.

¹⁰R. Sarkar and A. Chatterjee, Phys. Letters 30B, 313 (1969); Phys. Rev. C 1, 619 (1970); 4, 944 (1971); A. Chatterjee, International Atomic Energy Agency Report No. INDC-7/U (unpublished), p. 145; R. Sarkar and A. Chatterjee, in *Proceedings of the International Conference on Statistical Properties of Nuclei, Albany, 23-27 August 1971*, edited by J. B. Garg (Plenum, New York, 1972), p. 663.

¹¹S. Chatterjee, Nucl. Phys. A143, 277 (1970); Ph.D. thesis, Calcutta University, 1971 (unpublished); S. Mukherjee and A. Chatterjee, in *Proceedings of the International Conference on Statistical Properties of Nuclei, Albany, 23-27 August 1971* (see Ref. 10), p. 663.

¹²R. Sarkar and A. Chatterjee, Phys. Letters 33B, 263 (1971).

¹³R. Sarkar, Ph.D. thesis, Calcutta University, 1971 (unpublished).

¹⁴S. K. Ghosh, S. Mukherjee, and A. Chatterjee, Phys. Letters 38B, 203 (1972).

¹⁵W. J. Swiatecki, Phys. Rev. 104, 993 (1956).

¹⁶E. Landau, *Differential and Integral Calculus*, translated by M. Hausner and M. Davis (Chelsea, New York, 1951), p. 306.

¹⁷U. Mosel and W. Greiner, private communications;

Z. Physik 217, 256 (1969); 222, 261 (1970).

¹⁸S. K. Ghosh and A. Chatterjee, unpublished.

¹⁹N. Rosenzweig, private communication; Phys. Rev. 105, 950 (1957); 108, 817 (1957); N. Rosenzweig, L. M. Bollinger, L. L. Lee, and J. P. Schiffer, in *Proceedings of the Second United Nations International Conference on the Peaceful Uses of Atomic Energy, Geneva, Switzerland, 1958* (United Nations, Geneva, Switzerland, 1958), p. 11.

²⁰S. T. Belyaev, Kgl. Danske Videnskab. Selskab, Mat.-Fys. Medd. 31, No. 11 (1959).

²¹D. R. Bès, Kgl. Danske Videnskab. Selskab, Mat.-Fys. Medd. 33, No. 2 (1961).

²²A. A. Ross, Phys. Rev. 108, 720 (1957).

²³D. W. Lang, Nucl. Phys. 26, 434 (1961); 42, 353 (1963).

²⁴A. Chatterjee, Nucl. Phys. 47, 511 (1963); 49, 686 (1963).

²⁵A. Chatterjee, Bull. Am. Phys. Soc. 9, 170 (1964); Phys. Rev. 134, B374 (1964); Nucl. Phys. 60, 273 (1964); in *Proceedings of the International Conference on the Study of Nuclear Structure with Neutrons, Antwerp, Belgium, 1965*, edited by M. Nève de Mevergnies, P. Van Assche, and J. Vervier (North-Holland, Amsterdam, 1966), p. 543.

²⁶P. V. Rao and R. W. Fink, Phys. Rev. 154, 1023 (1967).

²⁷N. K. Majumdar and A. Chatterjee, Nucl. Phys. 41, 192 (1963).

²⁸A. V. Malyshev, Zh. Eksperim. i Teor. Fiz. 45, 316 (1963) [transl.: Soviet Phys.-JETP 18, 221 (1964)]; in *Proceedings of the International Conference on the Study of Nuclear Structure with Neutrons, Antwerp, Belgium, 1965* (see Ref. 25), p. 236.

²⁹A. Gilbert and A. G. W. Cameron, Can. J. Phys. 43, 1446 (1965).

³⁰A. G. W. Cameron and R. M. Elkin, Can. J. Phys. 43, 1288 (1965).

³¹P. E. Nemirovskii and Yu. V. Adamchuk, Nucl. Phys. 39, 551 (1962).

³²B. L. Cohen, *Concepts of Nuclear Physics* (McGraw-Hill, New York, 1971), p. 154.

³³N. Cindro, Rev. Mod. Phys. 38, 391 (1966).

³⁴P. A. Seeger, Los Alamos Report No. LA-DC-8950, 1967 (unpublished); P. A. Seeger and R. C. Perisho, Los Alamos Report No. LA-3751, 1967 (unpublished).

³⁵E. Rost, Phys. Letters 26B, 184 (1967).

³⁶S. G. Nilsson, R. Nix, A. Sobiczewski, Z. Szymanski, S. Wycech, C. Gustafson, and P. Möller, Nucl. Phys.

A115, 545 (1968); S. G. Nilsson, C. F. Tsang, A. Sobiczewski, Z. Szymanski, S. Wycech, C. Gustafson, I.-L. Lamm, P. Möller, and B. Nilsson, Nucl. Phys. A131, 1 (1969); A. Sobiczewski, Z. Szymanski, S. Wycech, S. G. Nilsson, J. R. Nix, C. F. Tsang, C. Gustafson, P. Möller, and B. Nilsson, Nucl. Phys. A131, 67 (1969).

³⁷S. K. Ghosh and A. Chatterjee, in Proceedings of the International Conference on Nuclear Structure Study with Neutrons, Budapest, 31 July-5 August 1972 (unpublished), p. 182.

³⁸G. T. Seaborg, Ann. Rev. Nucl. Sci. 18, 53 (1968).